Energy & Environmental Science

www.rsc.org/ees

Volume 6 | Number 5 | May 2013 | Pages 1341–1642

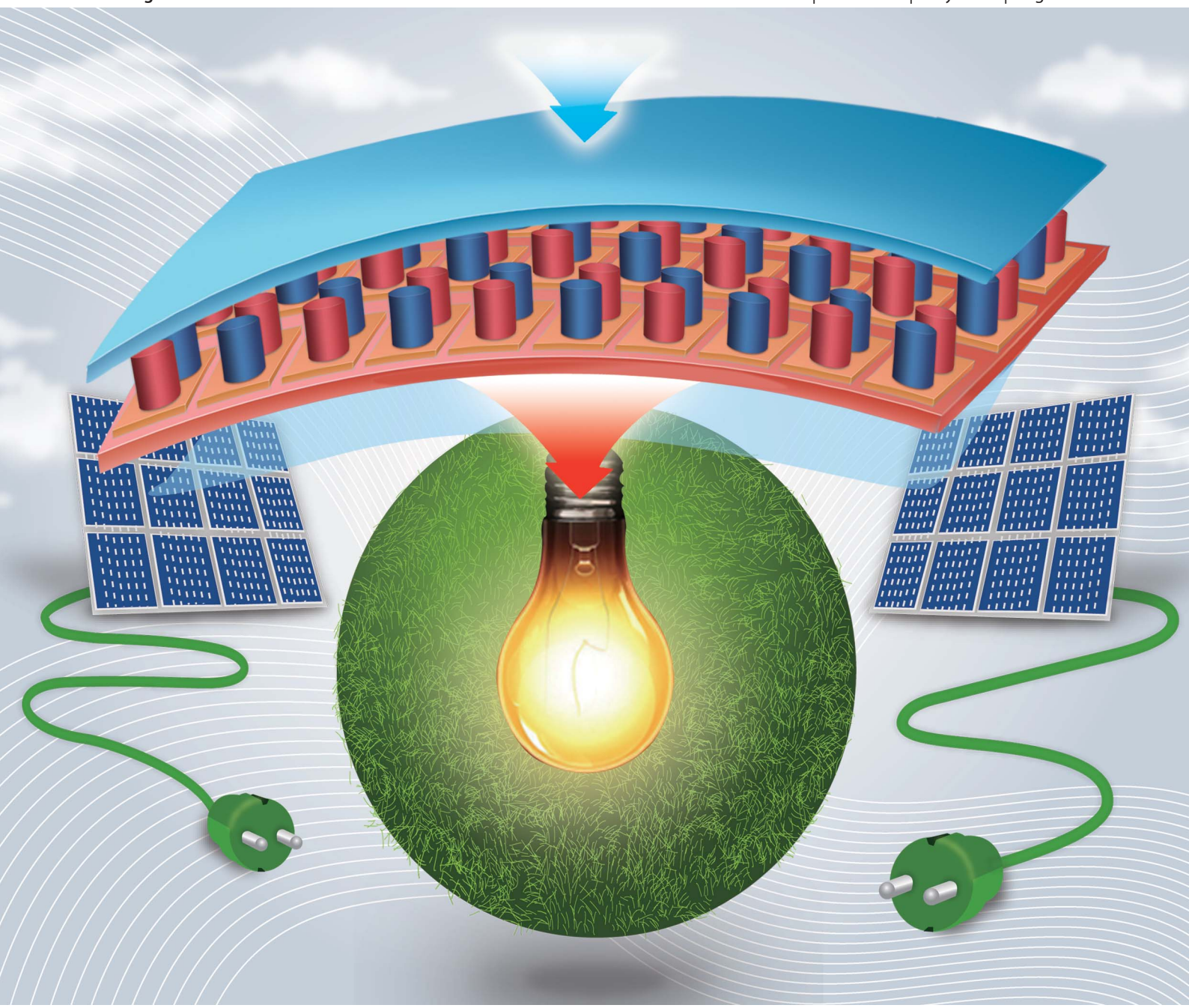

ISSN 1754-5692

RSC Publishing

REVIEW ARTICLE

Lin *et al.*

Towards high-performance polymer-based thermoelectric materials

1754-5692(2013)6:5;1-#

Energy & Environmental Science

RSC Publishing

REVIEW

View Article Online
View Journal | View Issue

Towards high-performance polymer-based thermoelectric materials

Cite this: *Energy Environ. Sci.*, 2013, **6**, 1352

Ming He,[a] Feng Qiu[a] and Zhiqun Lin*[b]

Received 26th November 2012
Accepted 11th January 2013

DOI: 10.1039/c3ee24193a

www.rsc.org/ees

Thermoelectric materials have garnered considerable attention due to their unique ability to directly convert heat to electricity and *vice versa*. Polymers carry many intrinsic advantages such as low thermal conductivity, solution processability, and roll-to-roll production for fabricating high-performance, lightweight, and flexible thermoelectric modules. In this review, we highlight recent advances in the preparation, modification and optimization of polymer thermoelectric materials, focusing especially on the current state-of-the-art strategies to minimize the thermal conductivity and maximize the power factor, and finally provide an outlook on the future development of this field.

Broader context

The growth of global industry and population has led to the demand for enormous energy, but the supply of conventional energy sources such as fossil oil, coal and natural gas is limited. One route to relieving the energy pressure caused by the increasing combustion of fossil fuels is to recycle waste heat by converting it into electricity. To this end, thermoelectric materials have been widely recognized as a simple and eco-friendly energy conversion means due to their unique ability to directly convert heat to electricity without any moving parts or bulk fluids. A good thermoelectric material requires a high Seebeck coefficient, high electrical conductivity and low thermal conductivity. In addition to inorganic semiconductors, polymers are potential candidates for high-performance thermoelectric applications due to their intrinsically low thermal conductivity. Moreover, polymer-based thermoelectric materials capitalize on the advantages peculiar to polymers, such as low cost, processability, flexibility, light weight, roll-to-roll production and large area, which are beneficial for the development of personal, portable, and flexible thermoelectric modules. In this review, recent advances in the preparation, modification and optimization of polymer thermoelectric materials are highlighted, and an outlook on the future development of this field is provided.

1 Introduction

Thermoelectric materials that enable the direct conversion between heat and electricity have received much attention as a promising route to developing power generation and cooling refrigeration without any moving parts or bulk fluids.[1–6] The working principle of thermoelectricity is associated with three fundamental effects, including: (1) the Seebeck effect, also referred to as the thermopower, in which an electrical potential is produced within a single conductor that is subjected to a temperature gradient; (2) the Peltier effect, in which a temperature difference is created at the junctions of two dissimilar conductors when an electric current crosses; and (3) the Thomson effect, in which the heat content within a single conductor is changed in a temperature gradient while an electric current passes through it.[7,8] Although these thermoelectric effects were independently discovered, they can be correlated through the Kelvin relationship that describes the basic thermoelectric behaviors as follows:[9–11]

$$\vec{i} = \sigma(\vec{E} - \alpha\vec{\nabla}T)$$

$$\vec{q} = \alpha T\vec{i} - \lambda\vec{\nabla}T$$

where i is the electric current density, q is the heat current density, E is the electric field, σ is the electrical conductivity, α is the Seebeck coefficient, λ is the thermal conductivity at zero electric field, and T is the absolute temperature. The coefficients (*i.e.*, α, σ, and λ) in the Kelvin relationship connect the electric and heat current changes with the electric field and temperature gradient,[12] in which the Seebeck effect α acts as the driving force for electric currents to generate the Peltier and Thomson effects in electrical circuits.[7,13]

The energy conversion efficiency of thermoelectric materials is quantified by the dimensionless figure-of-merit $ZT = \sigma\alpha^2T/\kappa$, where σ is the electrical conductivity, α is the Seebeck coefficient, κ is the thermal conductivity and T is the absolute temperature. The thermoelectric power factor P is calculated from the electrical conductivity and Seebeck coefficient where $P = \sigma\alpha^2$. A high-performance thermoelectric material requires (1) a high Seebeck coefficient to push the energy conversion of heat to electricity or electricity to cooling,[14–17] (2) a high electrical conductivity to reduce Joule heating,[18–20] and (3) a low thermal conductivity to prevent thermal shorting.[21–24] However,

[a]*State Key Laboratory of Molecular Engineering of Polymers, Department of Macromolecular Science, Fudan University, Shanghai, 200433, China*
[b]*School of Materials Science and Engineering, Georgia Institute of Technology, Atlanta, GA, 30332, USA. E-mail: zhiqun.lin@mse.gatech.edu*

the strong interdependence of these three parameters (*i.e.*, increasing σ is usually accompanied by an increased κ and a decreased α) imposes restrictions on maximizing *ZT* in homogeneous bulk materials.[25] To date, bulk thermoelectric materials only exhibit the best *ZT* of ~1 at 300 K, corresponding to the Carnot efficiency of ~10%. The *ZT* of at least 4 operating at the Carnot efficiency of ~30% is, however, needed for household appliances.[26]

Recent advances in the preparation and engineering of inorganic nanostructures greatly render the improvement of *ZT* by utilizing nanostructured inorganics such as phonon-blocking/electron-transmitting thin-film superlattices,[27–30] quantum-dot superlattices,[31–34] and nanoscale inclusions in bulk materials.[35,36] To date, most high *ZT* values have been achieved by preferentially reducing the thermal conductivity through the phonon scattering within superlattices or nanoinclusions, which removes localized heat fluxes without the loss of power factor,[37–39] resulting in a low thermal conductivity (*i.e.*, 1.1–1.5 W m^{-1} K^{-1}) comparable with that of amorphous solids, and thus the $ZT > 2$ at ~300 K.[27] Moreover, the energy-filtering effect within inorganic nanostructures can independently increase the Seebeck coefficient without greatly suppressing electrical conductivity,[40–44] providing an additional strategy to improve the *ZT*. However, these complex inorganic nanostructures are generally prepared by either the ball-milling, melt-spinning or the molecular beam epitaxy method that involves high-temperature, long-term and high-cost fabrication processes.

The intrinsically low thermal conductivity of polymers, which is about 1–3 orders of magnitude lower than that of inorganics,[45,46] make polymers to stand out as a potential candidate for high-performance thermoelectric applications. More importantly, the thermal conductivity of polymers depends marginally on chemical compositions, and typically lies in the range of 0.1–1 W m^{-1} K^{-1} in both conductive and insulating polymers,[46–50] thereby offering the expanded flexibility for realizing high-performance thermoelectric architectures *via* tuning power factor without heavily influencing thermal conductivity. In addition, these thermoelectric materials capitalize on the advantages peculiar to polymers, such as low cost, solution processability, flexibility, light weight, large area and roll-to-roll production, coinciding well with the requirements of future electronics that gear toward personal and portable polymer-based flexible electronics.[51–56]

Despite the low thermal conductivity, the electrical conductivity of polymer thermoelectric materials spans a very broad range from 10^{-8} S cm^{-1} to 10^{4} S cm^{-1}, and the Seebeck coefficient ranges from 10 μV K^{-1} to 1×10^{3} μV K^{-1}.[57–59] Similar to their inorganic counterparts, the electrical conductivity and the Seebeck coefficient of polymers are strongly correlated with the general tradeoff relationship, in which a higher electrical

Ming He received his PhD degree in Polymer Chemistry and Physics from Fudan University of China in 2011 under the supervision of Professor Feng Qiu. He worked with Professor Zhiqun Lin at Iowa State University of USA as a visiting student from 2009 to 2011. He is currently a postdoctoral researcher at Fudan University. His research interests include conjugated polymers, block copolymers, quantum dots, polymer solar cells, dye-sensitized solar cells, graphene electrode materials, and thermoelectric nanocomposites.

Feng Qiu received his Master degree in Engineering from Shanghai Institute of Metallurgy, Chinese Academy of Sciences in 1995, and his PhD degree in Polymer Chemistry and Physics from Fudan University in 1998. He was a postdoctoral research associate at University of Pittsburgh. In 2001 he joined Fudan University as an Associate Professor at the Department of Macromolecular Science, and was promoted to Professor in 2003. His research activities primarily involve the equilibrium and dynamical properties of complex block copolymers, polymer solutions, thin films, and graphene. He received China National Funds for Distinguished Young Scientists in 2006.

Zhiqun Lin received his Master degree in Macromolecular Science from Fudan University, Shanghai in 1998, and his PhD degree in Polymer Science and Engineering from UMass, Amherst in 2002. He was a postdoctoral associate at UIUC. He joined the Department of Materials Science and Engineering at Iowa State University in 2004, and was promoted to Associate Professor in 2010. He moved to Georgia Institute of Technology in 2011. His research interests include polymer solar cells, dye-sensitized solar cells, semiconductor organic–inorganic nanocomposites, photocatalysis, quantum dots (rods), conjugated polymers, block copolymers, polymer blends, hierarchical structure formation and assembly, surface and interfacial properties, multifunctional nanocrystals, and Janus nanostructures. He is a recipient of an NSF Career Award.

conductivity usually accompanies a lower Seebeck coefficient.[60] This can be explained by the position of the Fermi level in the energy band: a high doping level is believed to move the Fermi level close to the conduction band edge, thus reducing the transport energy of charge carriers.[9,61] The ability to balance the tradeoff relationship of the electrical conductivity and Seebeck coefficient is therefore crucial for promoting the power factor and thus the *ZT* of thermoelectric materials. For more details on the theoretical analysis and mechanism of polymer thermoelectric materials, the reader is referred to two recent Perspectives in Energy & Environmental Science.[9,62]

In this review, we aim to summarize recent progresses on the preparation, modification and optimization of polymer thermoelectric materials from an experimental viewpoint; highlight the current state-of-the-art strategies to minimize the thermal conductivity, maximize the power factor, and consequently improve the *ZT*; and finally provide an outlook on the future development of polymer thermoelectric materials.

2 Conductive polymers

2.1 Doping for an enhanced power factor

The increase of the power factor has been recognized as the key strategy in enhancing the *ZT* of conductive polymers given that their thermal conductivities are usually as low as those of amorphous solids. Pristine conductive polymers often possess a high Seebeck coefficient in the range of 1×10^2 to 5×10^3 $\mu V\ K^{-1}$,[57–59] which is possibly due to the electron–phonon scattering in the crystalline grains and the electron–phonon coupling in the insulating regime of conductive polymers.[9,57] The Seebeck coefficient originated from the electron–phonon coupling in pristine pentacene was estimated to be $265 \pm 40\ \mu V\ K^{-1}$.[63] On the other hand, the carrier concentration in pristine conductive polymers is too low to form an effective charge transport, usually leading to poor electrical conductivity below 10^{-8} S cm^{-1} and power factor below 1 $\mu W\ m^{-1}\ K^{-2}$.

In this context, doping conductive polymers to yield an increased electrical conductivity are widely employed.[64,65] For pristine conductive polymers, the charge transport is mostly dominated by phonon-assisted hopping between polymer chains, leading intrinsically to a very low carrier concentration and thus a poor electrical conductivity. In a doping process, extra charge carriers are introduced into the polymer chains, resulting in the formation of solitons, polarons and dipolarons responsible for charge transport along intra- or inter-chains.[66] The introduction of extra charge carriers can be realized by either chemical or electrochemical doping methods. A series of doping agents (*e.g.*, iodine, ferric trichloride, benzenesulfonic, camphor sulfonic acid, *etc.*) have been well explored.[67] As a representative conductive polymer, polyacetylene has been greatly studied since it was discovered in 1977.[68] For iodine-doped polyacetylenes, the electrical conductivity can reach as high as $\sim 1.0 \times 10^4$ S cm^{-1} with a Seebeck coefficient of $\sim 20\ \mu V\ K^{-1}$, and thus a highest power factor of 400 $\mu W\ m^{-1}\ K^{-2}$ at 300 K.[58,69] However, further attempts to improve the power factor are restricted by this relatively low Seebeck coefficient as the value of 1.0×10^4 S cm^{-1} is almost the maximum electrical conductivity for polyacetylenes. Although an extremely high Seebeck coefficient of 1077 $\mu V\ K^{-1}$ was obtained in $MoCl_5$-doped polyacetylenes, the electrical conductivity was found to be very low (*i.e.*, ~ 0.001 S cm^{-1}) due to the tradeoff relationship.[70] This competing trend of electrical conductivity and Seebeck coefficient can be ascribed to the movement of the Fermi level close to the conduction band gap due to doping, which reduces the transport energy of charge carriers, and in turn a reduced Seebeck coefficient.[9] Due to the disordered structures of conductive polymers, their density of states (DOS) is Gaussian, and progressively filled upon doping.[71] Therefore, the Seebeck coefficient that describes the ability of heat to drive charge carriers from a hot region to a cool region must be expressed from the weighted average of energy difference between the conduction band and the Fermi level.[62] The extra carrier concentrations introduced by doping is accompanied by the displacement of the Fermi level moving close to the conduction band, resulting in the decrease of the Seebeck coefficient. Therefore, it is clear that the doping level has to be delicately controlled to balance the electrical conductivity and Seebeck coefficient for a maximum power factor. Similar to inorganic thermoelectric materials, the nanostructure of conductive polymers may provide new opportunities to overcome the trade-off relationship benefiting from the quantum-confinement effect and the DOS change.[25]

2.2 Synthesis of new complex polymers

It is noteworthy that other conventional conductive polymers such as polyaniline, polypyrrole, polythiophene, and polyphenylene typically exhibit an even lower power factor than that of heavily doped polyacetylenes.[59] New conjugated polymers and copolymers were then explored to challenge the thermoelectric performance limits of polymers. A series of carbazole-based polymers with the donor–acceptor nature were synthesized by the Suzuki coupling, exhibiting an electrical conductivity up to 500 S cm^{-1} and a relatively high Seebeck coefficient up to 70 $\mu V\ K^{-1}$ in the doped films; a maximum power factor of 19 $\mu W\ m^{-1}\ K^{-2}$ was obtained by compromising these two parameters (*i.e.*, electrical conductivity and Seebeck coefficient).[72]

Poly(3,4-ethylenedioxythiophene) (PEDOT)-doped with polystyrene sulphonic acid (PSS) has been largely utilized as the electrode film in organic electronics due to its excellent electrical conductivity, solution processability, and environmental stability.[73–77] The *ZT* of pure PEDOT:PSS (*i.e.*, 0.0017) is comparable to that of conventional conductive polymers;[78] it can be improved up to 0.024 by the addition of high-boiling solvents (*i.e.*, dimethyl formamide, dimethyl sulfoxide, urea) to increase the electrical conductivity from ~ 10 S cm^{-1} to ~ 400 S cm^{-1} without changing the Seebeck coefficient too much.[79–82] The breakthrough was then achieved by replacing the polymer anion (*i.e.*, PSS) with a small-molecular anion (*i.e.*, tosylate), resulting in an enhanced electrical conductivity over 1000 S cm^{-1} due to the reduction of insulating polyanion phases (Fig. 1a).[83] The electrical conductivity and Seebeck coefficient of PEDOT:tosylate can be optimized by controlling the oxidation level during the polymerization. A highest *ZT* of 0.25 was

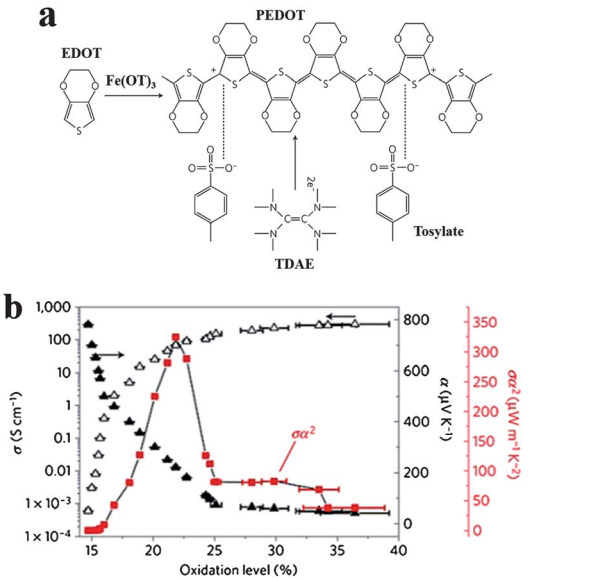

Fig. 1 (a) Sketch of the oxidative polymerization of EDOT by iron tosylate that creates the oxidized form of PEDOT. When exposed to the TDAE vapor, the tosylate-doped PEDOT can be reduced into neutral ones. (b) Seebeck coefficient α (filled triangles), electrical conductivity σ (open triangles) and the corresponding power factor $\sigma\alpha^2$ (red squares) as a function of the oxidation level. Adapted with permission from ref. 83, Copyright© 2011 Nature Publishing Group.

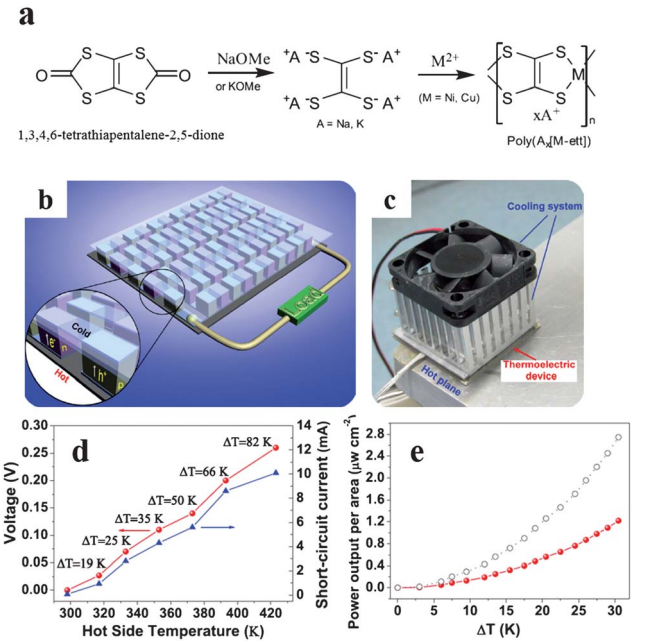

Fig. 2 (a) Scheme of the synthetic route to poly[A_x(M–ett)]s (ett = 1,1,2,2-ethenetetrathiolate). (b) Module structure. (c) Photograph of the module and the measurement system with a hot plane and cooling fan. (d) The output voltage and short-circuit current at various hot side temperatures (T_{hot}) and temperature gradient (ΔT). (e) Maximum power output per area of the module. Adapted with permission from ref. 84, Copyright© 2012 Wiley-VCH.

obtained at room temperature, which is the highest *ZT* value ever reported in polymer thermoelectric materials (Fig. 1b).[83]

Very recently, the thermoelectric properties of poly[A_x(A–ett)]s (ett = 1,1,2,2-ethenetetrathiolate) have been studied (Fig. 2a): the p-type poly[Cu_x(Cu–ett)] exhibited a best *ZT* of 0.014 at 380 K with an electrical conductivity of ~15 S cm^{-1}, a Seebeck coefficient of 80 μV K^{-1} and a thermal conductivity of 0.45 W K^{-1} m^{-1}; the *n*-type poly[K_x(Ni–ett)] showed a best *ZT* of 0.2 at 440 K with an electrical conductivity of ~60 S cm^{-1}, a Seebeck coefficient of −150 μV K^{-1} and a thermal conductivity of 0.25 W m^{-1} K^{-1}.[84] Moreover, the thermoelectric module based on the p-type poly[Cu_x(Cu–ett)] and n-type poly[Na_x(Ni–ett)] (*i.e.*, *ZT* of 0.1 at 440 K) was built (Fig. 2b and c). The module worked very well as a power generator; an open voltage of 0.26 V and a short-circuit current of 10.1 mA were produced when the temperature gradient reached 82 K (Fig. 2d). A maximum output power of 1.2 μW cm^{-2} was obtained at a temperature gradient of 30 K when the temperature of the cold side was maintained at room temperature (Fig. 2e).[84]

2.3 Tuning molecular conformations

It is well known that the semiconductor properties of conductive polymers also depend crucially on the physical conformation of polymer chains, which can self-assemble into various molecular-stacking structures such as nanowires, nanorings, and nanosheets *via* the π–π interactions.[85] In particular, one-dimensional (1D) stacking of conductive polymer chains is probably beneficial for a low thermal conductivity due to the interface-phonon scattering, an excellent electrical conductivity due to the highly oriented chain alignment, and a large Seebeck coefficient due to the enhanced density of state near the conduction band edge.[86–88] The PEDOT nanowires with the width of 150–580 nm, the thickness of 40–90 nm and the length of 200 μm were prepared using the lithographically patterned electrodeposition process. These n-type semiconductor nanowire arrays displayed a high Seebeck coefficient of −74 μV with a high electrical conductivity of 16.8 S cm^{-1}, in comparison to a Seebeck coefficient of −48 μV and an electrical conductivity of 11.1 S cm^{-1} in the conventional PEDOT films.[89]

3 Polymer nanocomposites

3.1 Polymer–carbon nanotube thermoelectric nanocomposites

Polymer-based thermoelectric nanocomposites are complimented by the combination of an extensive set of advantageous characteristics from polymers and nanofillers, that is, low thermal conductivity, solution processability, and flexibility of polymers, in conjunction with the high power factor of nanofillers. Among various nanofillers, carbon nanotubes (CNTs) are widely recognized as one of the most effective fillers to enhance the electrical conductivity of the polymer matrix due to their extremely high charge transport over long lengths without significant interruption.[90,91] Two strategies are often utilized to prepare polymer–CNT nanocomposites, namely, mixing nanofillers with the polymer matrix, and confining polymer chains on CNT templates *via* the π–π interactions.[92]

A low mixing content of CNTs is crucial to realize a high electrical conductivity without inducing a high thermal

conductivity in the polymer matrix.[93] Through a very slow drying process under ambient conditions, CNTs can form a three-dimensional (3D) network structure within an insulating poly(vinyl acetate) (PVAc) emulsion matrix, in which CNTs were wrapped by the PVAc particles rather than randomly distributed in the nanocomposites.[94] The electrical conductivity of the resulting nanocomposites increased with the addition of more CNTs, yielding a maximum of ~48 S cm^{-1}, which was much higher than that of conventional polymer–CNT nanocomposites at similar CNT concentrations. Quite intriguingly, the Seebeck coefficient (*i.e.*, 40–50 μV K^{-1}) and thermal conductivity (*i.e.*, 0.2–0.3 W m^{-1} K^{-1}) were nearly constant with the addition of CNTs, thus resulting in the best *ZT* of ~0.006 at a CNT concentration of 20 wt% at 300 K.[94] Moreover, the thermal conductivity of polymer–CNT nanocomposites can be reduced to be lower than that of the polymer matrix by using 3D porous sponge-like multiwall CNTs as the nanofillers, which was synthesized by chemical vapor deposition and possessed the lowest thermal conductivity of 0.035 W m^{-1} K^{-1} among all kinds of CNTs.[95]

The connecting junctions between CNTs in nanocomposites were found to play an important role in enhancing the electrical conductivity without increasing the thermal conductivity of polymer–CNT nanocomposites (Fig. 3a).[96] When blended in a polymer matrix, CNTs were connected in series by van der Waals force due to the presence of conductive polymer particles at the junctions, whose molecular vibrational spectra are mismatched with that of CNTs, thereby impeding the phonon transport at the junctions.[94,96,97] The replacement of the insulating PVAc matrix with conductive polymer PEDOT:PSS increased the maximum electrical conductivity of nanocomposites from ~48 S cm^{-1} in PVAc–CNT nanocomposites to ~1350 S cm^{-1} in PEDOT:PSS–CNT nanocomposites, while the Seebeck coefficient and thermal conductivity were retained at ~30 μV K^{-1} and ~0.4 W m^{-1} K^{-1}, respectively (Fig. 3b), suggesting that these strongly correlated thermoelectric parameters may be decoupled in polymer nanocomposites.[96] It is worth noting that the electrical conductivity and Seebeck coefficient are often strongly correlated in conventional thermoelectric bulk materials, and the decoupling of these two parameters has only been observed in few complex inorganic nanostructures *via* the carrier-pocket engineering,[98,99] carrier energy-filtering effect,[41,44,100,101] and semimetal–semiconductor transition.[25]

In addition to PEDOT:PSS–CNT nanocomposites, the decoupling effect associated with the enhancement of Seebeck coefficient was also observed in polyaniline–CNT nanocomposites, in which the Seebeck coefficient of nanocomposites was remarkably increased to a maximum value of 28.6 μV K^{-1} at 350 K as compared to those of polyaniline (*i.e.*, 2.74 μV K^{-1}) and CNT (*i.e.*, 12.2 μV K^{-1}) bulk samples (Fig. 4).[102] This unexpected increase of Seebeck coefficient was possibly due to the energy-filtering effect at the polyaniline–CNT interface, where appropriate potential boundary barriers preferentially allowed the carriers with the higher energy to pass, thereby increasing the mean carrier energy in the flow and thus an increased Seebeck coefficient.[102]

The attempt to simultaneously increase the electrical conductivity and Seebeck coefficient in polymer thermoelectric nanocomposites may also be realized by improving the carrier mobility while maintaining the carrier concentration of nanocomposites, in which CNTs were used as a template to guide the self-assembly of conductive polymers into more ordered crystalline alignments *via* the π–π interactions (Fig. 5a and b).[103–105] For example, in comparison with pure polyanilines, ordered

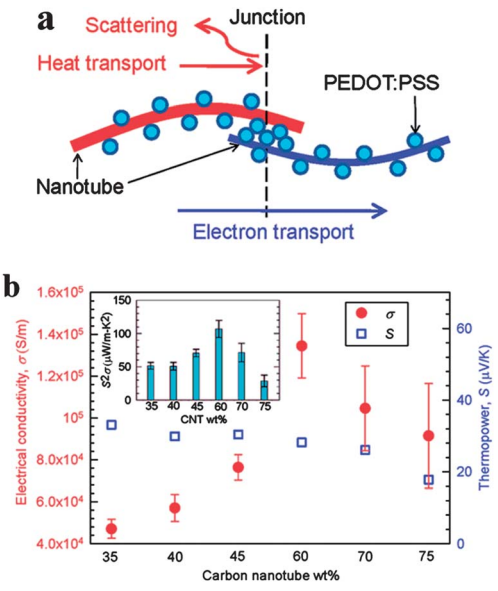

Fig. 3 (a) Schematic illustration of the junctions of carbon nanotubes coated by PEDOT:PSS particles. (b) Electrical conductivities σ and Seebeck coefficient α of the composites at different nanotube concentrations. The inset shows the thermoelectric power factor $\sigma\alpha^2$. Adapted with permission from ref. 96, Copyright© 2011 American Chemical Society.

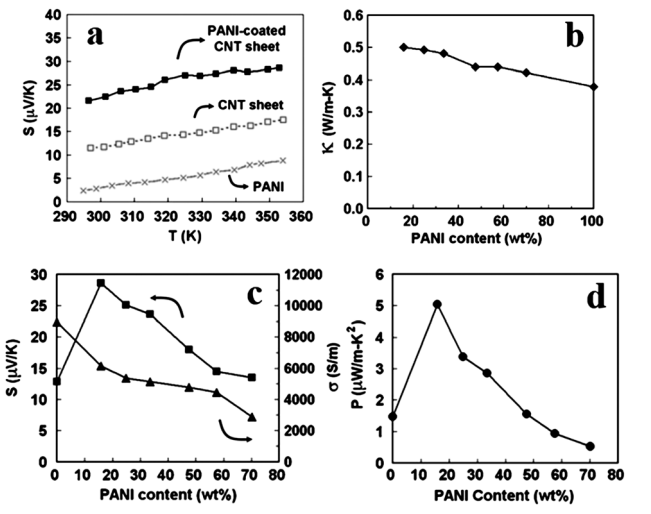

Fig. 4 (a) Seebeck coefficient as a function of temperature for polyaniline–CNT nanocomposites. (b) Thermal conductivity of polyaniline–CNT nanocomposites as a function of polyaniline content. (c) Seebeck coefficient α, electrical conductivity σ (open triangles) and (d) the corresponding power factor $\sigma\alpha^2$ as a function of polyaniline content. Adapted with permission from ref. 102, Copyright© 2010 Wiley-VCH.

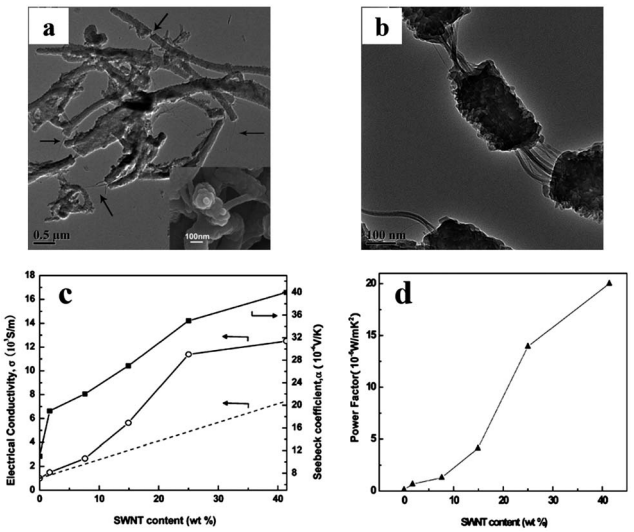

Fig. 5 (a and b) TEM images of polyaniline–single-walled nanotube (SWNT) composites with 25 wt% SWNT. Inset of (a) is the top view SEM of the nanocomposite. (c) Seebeck coefficient, electrical conductivity, and (d) power factor of polyaniline–SWNT composites at different SWNT contents. The dashed line is the calculated electrical conductivity based on the particle mixture rule. Adapted with permission from ref. 103, Copyright© 2010 American Chemical Society.

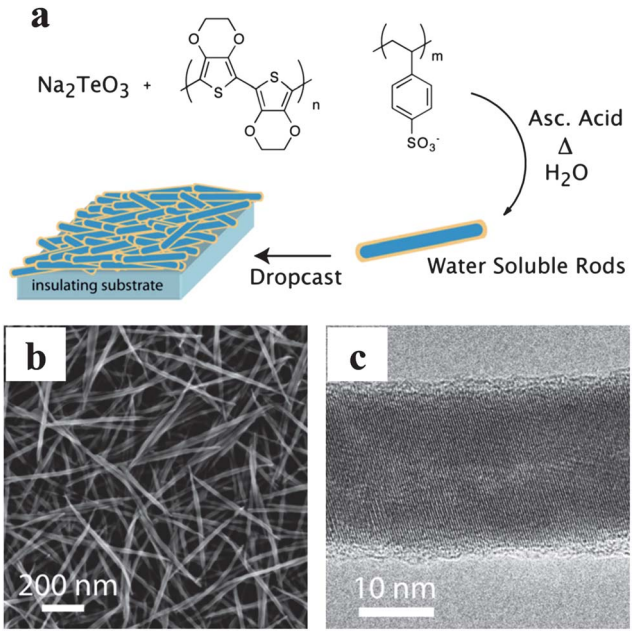

Fig. 6 (a) Synthesis of PEDOT:PSS passivated Te nanorods, followed by the formation of smooth nanocomposite films during the solution casting. (b) SEM image of a drop-cast composite nanorod film. (c) TEM image showing the crystalline Te nanorod passivated with PEDOT:PSS. Adapted with permission from ref. 111, Copyright© 2010 American Chemical Society.

polyaniline structures attached onto the CNT surfaces rendered the increase of carrier mobility from 0.18 $cm^2\ V^{-1}\ s^{-1}$ to 0.97 $cm^2\ V^{-1}\ s^{-1}$, while the carrier concentration was retained in the range of 3×10^{20} cm^{-3} to 7×10^{20} cm^{-3}. Obviously, the increased carrier mobility was responsible for the improvement of electrical conductivity from ~10 S cm^{-1} to 125 S cm^{-1} and Seebeck coefficient from 11 to 40 μV K^{-1} (Fig. 5c and d), leading to the highest power factor of ~20 μW m^{-1} K^{-2} at the CNT concentration of 40 wt%.[103]

3.2 Polymer–inorganic thermoelectric nanocomposites

The fabrication of inorganic thermoelectric materials into large-area modules involves high-temperature, long-term and high-cost processes. Moreover, it is a grand challenge to integrate these rigid inorganic materials into unusual topologies to fit the geometrical requirements for an enhanced practical efficiency.[106] One of the most particularly attractive features of polymer–inorganic thermoelectric nanocomposites lies in the synergetic combination of the easy processability of polymers and the excellent thermoelectric performance of inorganic semiconductors. Among a variety of nanostructured inorganic thermoelectrics, Bi, Te, and Bi_2Te_3 nanostructures are highly favorable for mixing with the polymer matrix due to their high power factor at room temperature, facile synthesis, and solution-processed dispersion.[107–110] Recently, the highest *ZT* of polymer–inorganic thermoelectric nanocomposites have been demonstrated in PEDOT:PSS–Te nanorod composites (*i.e.*, *ZT* of ~0.1 at 300 K).[111] The *in situ* prepared nanocomposites exhibited a higher power factor than those of individual constituents, and possessed a low thermal conductivity comparable with that of the polymer matrix (Fig. 6a).[111] The nanocomposite film contained a continuous electrical network of nanoscale PEDOT:PSS–Te organic–inorganic interfaces (Fig. 6b), yielding an electrical conductivity of ~19 S cm^{-1}, as compared to that of 1.32 S cm^{-1} and 0.08 S cm^{-1} in pure PEDOT:PSS and Te, respectively. The improved power factor in PEDOT:PSS–Te nanocomposites was also attributed to the possibility of the energy-filtering effect at the Te nanorod surface passivated with PEDOT:PSS (Fig. 6c).

Notably, the energy-filtering approach was originally proposed for superlattices in inorganic thermoelectric materials where alternate energy barrier layers act as energy filters to substantially scatter low-energy carriers;[112] this concept was then extended to three-dimensional bulk inorganics where either nanoparticles or grain boundary interfaces play the role of energy filters.[43,100] Recently, it has been demonstrated that the organic–inorganic semiconductor interface in polymer–inorganic nanocomposites can also act as an energy filter, which was verified by characterizing the energy-dependent scattering parameter and the energy band structure of nanocomposites.[113] Fig. 7a shows a representative correlation between electrical conductivity and Seebeck coefficient in both P3HT and P3HT–Bi_2Te_3 nanocomposites, in which the P3HT matrix was doped by $FeCl_3$. In light of the tradeoff relationship noted above, the Seebeck coefficients of P3HT and P3HT–Bi_2Te_3 after doping progressively decreased from 450 μV K^{-1} to below 100 μV K^{-1} with the increased electrical conductivity. Interestingly, P3HT–Bi_2Te_3 nanocomposites readily displayed higher Seebeck coefficients than those of P3HT films in the range of high electrical conductivity (*i.e.*, σ > 200 S m^{-1}, Fig. 7a), thereby leading to markedly improved power factors in nanocomposites as compared to those of P3HT films. We note that the

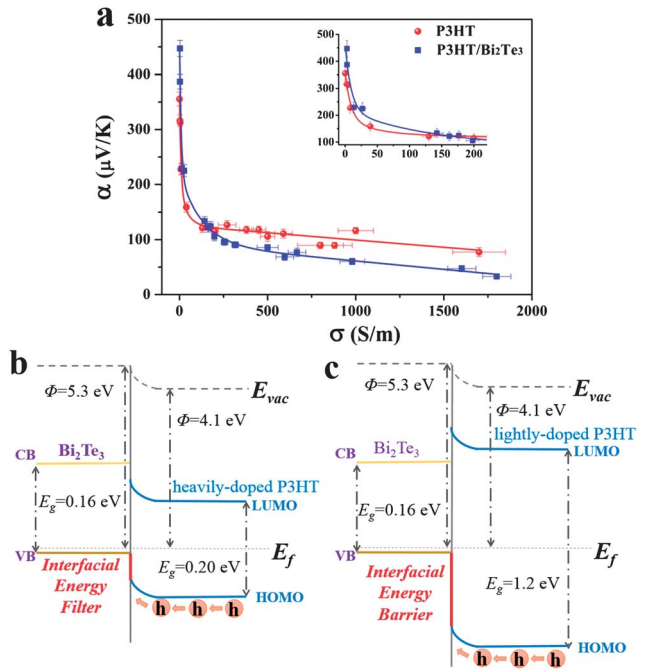

Fig. 7 (a) The correlation between the Seebeck coefficient α and the electrical conductivity σ in P3HT and P3HT–Bi_2Te_3 nanocomposites; the inset shows the close-up in the range of low electrical conductivity (*i.e.*, σ < 200 S m^{-1}). (b) The band diagram of P3HT–Bi_2Te_3 interface based on the heavily doped P3HT matrix. (c) The band diagram of the P3HT–Bi_2Te_3 interface based on the lightly doped P3HT matrix. Adapted with permission from ref. 113, Copyright© 2012 Royal Society of Chemistry.

enhancement of the Seebeck coefficient and power factor in P3HT–Bi_2Te_3 nanocomposites did not appear in the range of low electrical conductivity, indicating that a more complex mechanism rather than the tradeoff between these two parameters was responsible for the improved Seebeck coefficient in P3HT–Bi_2Te_3 nanocomposites.

By combining theoretical calculation and experimental characterization, a series of thermoelectric transport parameters (*i.e.*, the Fermi level, band gap, effective mass, carrier concentration, and energy-dependent scattering parameter) can be derived from the experimentally measured electrical conductivity, Seebeck coefficient and Hall coefficient,[14,31,114,115] clearly revealing the carrier energy-filtering effect at the P3HT–Bi_2Te_3 semiconductor interfaces (Fig. 7b and c). For the heavily doped P3HT matrix, an interfacial potential barrier of below 0.1 eV formed at the P3HT–Bi_2Te_3 interface to selectively scatter low-energy carriers rather than high-energy carriers; while the P3HT–Bi_2Te_3 interfaces in the lightly doped system probably acted as an energy barrier without the energy-filtering effect due to the large potential barrier and incompatible bandgaps of P3HT–Bi_2Te_3 nanocomposites.[113]

4 Conclusions and outlook

Despite recent exciting progress described above, the development of polymer thermoelectric materials is still in its infancy. To date, the maximum *ZT* of polymers (*i.e.*, 0.25) was obtained in tosylate-doped PEDOT at room temperature,[83] but it was only comparable to that of inorganic bulk thermoelectric materials. Promoting the *ZT* over 4 is still a grand challenging issue for all kinds of thermoelectric materials, at which the advantageous characteristics of polymer thermoelectric materials including low cost, solution processability, flexibility, light weight, and roll-to-roll production can be fully benefited and executed. We note that polymer thermoelectric materials will compete in future with inorganic thermoelectric materials mainly in cooling systems and low-temperature power generators, owing to a limited thermal stability of polymers (*i.e.*, roughly below 400 K). As for the high-temperature applications, polymers will hardly substitute for inorganic materials, such as the Si–Ge alloy or recently discovered $Yb_{14}MnSb_{11}$.[116,117] Polymer thermoelectric materials are more likely an extension of the application of the thermoelectric phenomenon rather than the replacement for the inorganic counterparts.

The efficiency of polymer thermoelectric materials is mainly restricted by the relatively low power factor in comparison to that of inorganics. In particular, the low Seebeck coefficient (below 20 μV K^{-1} in heavily doped conductive polymers) compromises the enhancement of electrical conductivity. An increased carrier mobility is regarded as the most promising route to improving the power factor.[118] Recent progress in the design of functional conductive polymers has rendered a high carrier mobility at definite energy levels by delicately tailoring molecular structures and device configurations.[119] Furthermore, the creation of additional energy states in polymer blends by doping with an additive can also probably generate more regimes between the Fermi level and the conduction band edge,[119] leading to the simultaneous increase of electrical conductivity and Seebeck coefficient. The coupling effect of electrical and thermal conductivity is not beneficial to increasing the Seebeck coefficient, as a high thermal conductivity will reduce the entropy difference, which is the driving force for charge transport under thermal diffusion, through the electron–phonon interaction between the hot and cold regions. A high electrical conductivity but low thermal conductivity is favorable for an enhanced Seebeck coefficient, which recently has been realized in hybrid metal–polymer–metal thin-film devices, wherein the Ohmic metal–polymer contacts allow the formation of good electrical conductivity while the phonon scattering at metal–polymer interfaces minimizes the thermal conductivity.[120]

Crafting nanostructured inorganic thermoelectric materials has emerged as a general approach to enhance *ZT*,[5] and this should also be readily applicable to organic thermoelectric materials. An extremely high power factor was obtained in quasi-one-dimensional self-assembled organic molecular nanowires based on a rigorous theoretical evaluation, suggesting that the use of low-dimensional structures of conductive polymers can indeed be a promising direction to achieve high thermoelectric performance.[86] Moreover, rationally engineering the polymer–inorganic interface offers an alternative potentially viable route to improve thermoelectric performance; some of the concepts in inorganic nanostructures such as phonon scattering, carrier-energy-filtering, and carrier-pocket

engineering may also be adopted in polymer thermoelectric materials. Several important principles for constructing energy-filtering interfaces in polymer–inorganic nanocomposites can be suggested:[40,102,111,121] (1) intimate contact between polymers and nanoparticles to establish a well-controlled organic–inorganic interface, (2) similar work functions of polymers and nanoparticles to facilitate high-energy carriers transferring across the interface, (3) interfacial barrier height below 0.1 eV to selectively scatter low-energy carriers rather than high-energy carriers, (4) one-dimensional nanostructures to build effective potential barriers in a low filler concentration as compared to that of zero-dimensional nanoparticles.

Given the complexity of thermoelectric research, the judicious combination of experiments, theory and simulation is expected to be capable of suggesting feasible strategies for the optimization of polymer thermoelectric materials. To this end, studies on the thermoelectric mechanisms of polymers need be strengthened. Further elucidation on the electrical conductivity, thermal transport, and thermoelectric behavior of polymers will be beneficial to explore new concepts to promote the performance of organic thermoelectricity. Nonetheless, with the rapid progress being made in organic synthesis, polymer engineering, device fabrication, and theoretical modeling, polymer thermoelectric materials will remain as an extraordinarily active area for thermoelectric exploration and application.

Acknowledgements

M. H. gratefully acknowledges financial support from the China Postdoctoral Science Foundation (Grant no. 2011M500723 and 2012T50394). Z.L. gratefully acknowledges the support from Georgia Institute of Technology.

Notes and references

1 A. I. Hochbaum, R. K. Chen, R. D. Delgado, W. J. Liang, E. C. Garnett, M. Najarian, A. Majumdar and P. D. Yang, *Nature*, 2008, **451**, 163.
2 T. C. Harman, P. J. Taylor, M. P. Walsh and B. E. LaForge, *Science*, 2002, **297**, 2229.
3 B. C. Sales, D. Mandrus and R. K. Williams, *Science*, 1996, **272**, 1325.
4 L. E. Bell, *Science*, 2008, **321**, 1457.
5 J. R. Sootsman, D. Y. Chung and M. G. Kanatzidis, *Angew. Chem., Int. Ed.*, 2009, **48**, 8616.
6 A. J. Minnich, M. S. Dresselhaus, Z. F. Ren and G. Chen, *Energy Environ. Sci.*, 2009, **2**, 466.
7 D. M. Rowe, *CRC handbook of thermoelectrics*, CRC Press, Boca Raton, FL, 1995.
8 D. M. Rowe, *Thermoelectrics handbook: macro to nano*, CRC/Taylor & Francis, Boca Raton, 2006.
9 O. Bubnova and X. Crispin, *Energy Environ. Sci.*, 2012, **5**, 9345.
10 J. P. Heremans, C. M. Thrush and D. T. Morelli, *Phys. Rev. Lett.*, 2001, **86**, 2098.
11 M. J. Lampinen, *J. Appl. Phys.*, 1991, **69**, 4318.
12 E. H. Sondheimer, *Proc. R. Soc. London, Ser. A*, 1956, **234**, 391.
13 F. L. Bakker, A. Slachter, J. P. Adam and B. J. van Wees, *Phys. Rev. Lett.*, 2010, **105**, 136601.
14 J. P. Heremans, V. Jovovic, E. S. Toberer, A. Saramat, K. Kurosaki, A. Charoenphakdee, S. Yamanaka and G. J. Snyder, *Science*, 2008, **321**, 554.
15 H. Ohta, S. Kim, Y. Mune, T. Mizoguchi, K. Nomura, S. Ohta, T. Nomura, Y. Nakanishi, Y. Ikuhara, M. Hirano, H. Hosono and K. Koumoto, *Nat. Mater.*, 2007, **6**, 129.
16 P. Reddy, S. Y. Jang, R. A. Segalman and A. Majumdar, *Science*, 2007, **315**, 1568.
17 Y. Z. Pei, A. LaLonde, S. Iwanaga and G. J. Snyder, *Energy Environ. Sci.*, 2011, **4**, 2085.
18 C. Uher, J. Yang, S. Hu, D. T. Morelli and G. P. Meisner, *Phys. Rev. B: Condens. Matter Mater. Phys.*, 1999, **59**, 8615.
19 J. N. Coleman, M. Lotya, A. O'Neill, S. D. Bergin, P. J. King, U. Khan, K. Young, A. Gaucher, S. De, R. J. Smith, I. V. Shvets, S. K. Arora, G. Stanton, H. Y. Kim, K. Lee, G. T. Kim, G. S. Duesberg, T. Hallam, J. J. Boland, J. J. Wang, J. F. Donegan, J. C. Grunlan, G. Moriarty, A. Shmeliov, R. J. Nicholls, J. M. Perkins, E. M. Grieveson, K. Theuwissen, D. W. McComb, P. D. Nellist and V. Nicolosi, *Science*, 2011, **331**, 568.
20 L. Shi, D. Y. Li, C. H. Yu, W. Y. Jang, D. Kim, Z. Yao, P. Kim and A. Majumdar, *J. Heat Transfer*, 2003, **125**, 881.
21 D. Vashaee and A. Shakouri, *Phys. Rev. Lett.*, 2004, **92**, 106103.
22 A. I. Boukai, Y. Bunimovich, J. Tahir-Kheli, J. K. Yu, W. A. Goddard and J. R. Heath, *Nature*, 2008, **451**, 168.
23 D. G. Cahill, W. K. Ford, K. E. Goodson, G. D. Mahan, A. Majumdar, H. J. Maris, R. Merlin and P. Sr, *J. Appl. Phys.*, 2003, **93**, 793.
24 J. Y. Tang, H. T. Wang, D. H. Lee, M. Fardy, Z. Y. Huo, T. P. Russell and P. D. Yang, *Nano Lett.*, 2010, **10**, 4279.
25 M. S. Dresselhaus, G. Chen, M. Y. Tang, R. G. Yang, H. Lee, D. Z. Wang, Z. F. Ren, J. P. Fleurial and P. Gogna, *Adv. Mater.*, 2007, **19**, 1043.
26 F. J. DiSalvo, *Science*, 1999, **285**, 703.
27 I. Chowdhury, R. Prasher, K. Lofgreen, G. Chrysler, S. Narasimhan, R. Mahajan, D. Koester, R. Alley and R. Venkatasubramanian, *Nat. Nanotechnol.*, 2009, **4**, 235.
28 R. Venkatasubramanian, *Phys. Rev. B: Condens. Matter Mater. Phys.*, 2000, **61**, 3091.
29 P. Hyldgaard and G. D. Mahan, *Phys. Rev. B: Condens. Matter Mater. Phys.*, 1997, **56**, 10754.
30 H. Bottner, G. Chen and R. Venkatasubramanian, *MRS Bull.*, 2006, **31**, 211.
31 J. P. Heremans, C. M. Thrush and D. T. Morelli, *Phys. Rev. B: Condens. Matter Mater. Phys.*, 2004, **70**, 115334.
32 R. Y. Wang, J. P. Feser, J. S. Lee, D. V. Talapin, R. Segalman and A. Majumdar, *Nano Lett.*, 2008, **8**, 2283.
33 P. Trocha and J. Barnas, *Phys. Rev. B: Condens. Matter Mater. Phys.*, 2012, **85**, 085408.
34 Z. W. Quan, Z. P. Luo, W. S. Loc, J. Zhang, Y. X. Wang, K. K. Yang, N. Porter, J. Lin, H. Wang and J. Y. Fang, *J. Am. Chem. Soc.*, 2011, **133**, 17590.

35 J. P. A. Makongo, D. K. Misra, X. Y. Zhou, A. Pant, M. R. Shabetai, X. L. Su, C. Uher, K. L. Stokes and P. F. P. Poudeu, *J. Am. Chem. Soc.*, 2011, **133**, 18843.
36 J. W. Simonson, D. Wu, W. J. Xie, T. M. Tritt and S. J. Poon, *Phys. Rev. B: Condens. Matter Mater. Phys.*, 2011, **83**, 235211.
37 J. K. Yu, S. Mitrovic, D. Tham, J. Varghese and J. R. Heath, *Nat. Nanotechnol.*, 2010, **5**, 718.
38 X. Shi, J. Yang, J. R. Salvador, M. F. Chi, J. Y. Cho, H. Wang, S. Q. Bai, J. H. Yang, W. Q. Zhang and L. D. Chen, *J. Am. Chem. Soc.*, 2011, **133**, 7837.
39 J. Q. He, J. Androulakis, M. G. Kanatzidis and V. P. Dravid, *Nano Lett.*, 2012, **12**, 343.
40 M. Zebarjadi, K. Esfarjani, M. S. Dresselhaus, Z. F. Ren and G. Chen, *Energy Environ. Sci.*, 2012, **5**, 5147.
41 D. K. Ko, Y. J. Kang and C. B. Murray, *Nano Lett.*, 2011, **11**, 2841.
42 M. Scheele, N. Oeschler, I. Veremchuk, S. O. Peters, A. Littig, A. Kornowski, C. Klinke and H. Weller, *ACS Nano*, 2011, **5**, 8541.
43 A. Soni, Y. Y. Zhao, L. G. Yu, M. K. K. Aik, M. S. Dresselhaus and Q. H. Xiong, *Nano Lett.*, 2012, **12**, 1203.
44 A. Soni, Y. Q. Shen, M. Yin, Y. Y. Zhao, L. G. Yu, X. Hu, Z. L. Dong, K. A. Khor, M. S. Dresselhaus and Q. H. Xiong, *Nano Lett.*, 2012, **12**, 4305.
45 Y. C. Zhou, L. Wang, H. Zhang, Y. Y. Bai, Y. J. Niu and H. Wang, *Appl. Phys. Lett.*, 2012, **101**, 021903.
46 Z. D. Han and A. Fina, *Prog. Polym. Sci.*, 2011, **36**, 914.
47 M. Alaghemandi, M. R. Gharib-Zahedi, E. Spohr and M. C. Bohm, *J. Phys. Chem. C*, 2012, **116**, 14115.
48 E. Kamseu, B. Nait-Ali, M. C. Bignozzi, C. Leonelli, S. Rossignol and D. S. Smith, *J. Eur. Ceram. Soc.*, 2012, **32**, 1593.
49 X. Y. Huang, T. Iizuka, P. K. Jiang, Y. Ohki and T. Tanaka, *J. Phys. Chem. C*, 2012, **116**, 13629.
50 H. Yan, N. Sada and N. Toshima, *J. Therm. Anal. Calorim.*, 2002, **69**, 881.
51 M. He, J. Ge, M. Fang, F. Qiu and Y. L. Yang, *Polymer*, 2010, **51**, 2236.
52 M. He, W. Han, J. Ge, Y. L. Yang, F. Qiu and Z. Q. Lin, *Energy Environ. Sci.*, 2011, **4**, 2894.
53 M. He, W. Han, J. Ge, W. J. Yu, Y. L. Yang, F. Qiu and Z. Q. Lin, *Nanoscale*, 2011, **3**, 3159.
54 M. He, F. Qiu and Z. Q. Lin, *J. Mater. Chem.*, 2011, **21**, 17039.
55 J. Ge, M. He, X. B. Yang, Z. Ye, X. F. Liu and F. Qiu, *J. Mater. Chem.*, 2012, **22**, 19213.
56 Z. L. Wang, *Adv. Mater.*, 2012, **24**, 280.
57 A. B. Kaiser, *Rep. Prog. Phys.*, 2001, **64**, 1.
58 Y. Xuan, X. Liu, S. Desbief, P. Leclere, M. Fahlman, R. Lazzaroni, M. Berggren, J. Cornil, D. Emin and X. Crispin, *Phys. Rev. B: Condens. Matter Mater. Phys.*, 2010, **82**, 115454.
59 Y. Du, S. Z. Shen, K. F. Cai and P. S. Casey, *Prog. Polym. Sci.*, 2012, **37**, 820.
60 G. J. Snyder and E. S. Toberer, *Nat. Mater.*, 2008, **7**, 105.
61 D. K. Ko and C. B. Murray, *ACS Nano*, 2011, **5**, 4810.
62 T. O. Poehler and H. E. Katz, *Energy Environ. Sci.*, 2012, **5**, 8110.
63 A. von Muhlenen, N. Errien, M. Schaer, M. N. Bussac and L. Zuppiroli, *Phys. Rev. B: Condens. Matter Mater. Phys.*, 2007, **75**, 115338.
64 Y. Zhang, B. de Boer and P. W. M. Blom, *Phys. Rev. B: Condens. Matter Mater. Phys.*, 2010, **81**, 085201.
65 J. M. Lee, J. S. Park, S. H. Lee, H. Kim, S. Yoo and S. O. Kim, *Adv. Mater.*, 2011, **23**, 629.
66 J. L. Bredas and G. B. Street, *Acc. Chem. Res.*, 1985, **18**, 309.
67 B. P. Tripathi and V. K. Shahi, *Prog. Polym. Sci.*, 2011, **36**, 945.
68 C. K. Chiang, C. R. Fincher, Y. W. Park, A. J. Heeger, H. Shirakawa, E. J. Louis, S. C. Gau and A. G. Macdiarmid, *Phys. Rev. Lett.*, 1977, **39**, 1098.
69 A. B. Kaiser, *Adv. Mater.*, 2001, **13**, 927.
70 Y. W. Park, *Synth. Met.*, 1991, **45**, 173.
71 S. D. Baranovskii, I. P. Zvyagin, H. Cordes, S. Yamasaki and P. Thomas, *Phys. Status Solidi B*, 2002, **230**, 281.
72 R. B. Aich, N. Blouin, A. Bouchard and M. Leclerc, *Chem. Mater.*, 2009, **21**, 751.
73 A. M. Nardes, M. Kemerink, R. A. J. Janssen, J. A. M. Bastiaansen, N. M. M. Kiggen, B. M. W. Langeveld, A. van Breemen and M. M. de Kok, *Adv. Mater.*, 2007, **19**, 1196.
74 X. Crispin, F. L. E. Jakobsson, A. Crispin, P. C. M. Grim, P. Andersson, A. Volodin, C. van Haesendonck, M. Van der Auweraer, W. R. Salaneck and M. Berggren, *Chem. Mater.*, 2006, **18**, 4354.
75 A. M. Nardes, R. A. J. Janssen and M. Kemerink, *Adv. Funct. Mater.*, 2008, **18**, 865.
76 Y. H. Kim, C. Sachse, M. L. Machala, C. May, L. Muller-Meskamp and K. Leo, *Adv. Funct. Mater.*, 2011, **21**, 1076.
77 D. J. Lipomi, J. A. Lee, M. Vosgueritchian, B. C. K. Tee, J. A. Bolander and Z. A. Bao, *Chem. Mater.*, 2012, **24**, 373.
78 F. X. Jiang, J. K. Xu, B. Y. Lu, Y. Xie, R. J. Huang and L. F. Li, *Chin. Phys. Lett.*, 2008, **25**, 2202.
79 M. Scholdt, H. Do, J. Lang, A. Gall, A. Colsmann, U. Lemmer, J. D. Koenig, M. Winkler and H. Boettner, *J. Electron. Mater.*, 2010, **39**, 1589.
80 T. Stocker, A. Kohler and R. Moos, *J. Polym. Sci., Part B: Polym. Phys.*, 2012, **50**, 976.
81 F. F. Kong, C. C. Liu, J. K. Xu, Y. Huang, J. M. Wang and Z. Sun, *J. Electron. Mater.*, 2012, **41**, 2431.
82 C. C. Liu, B. Y. Lu, J. Yan, J. K. Xu, R. R. Yue, Z. J. Zhu, S. Y. Zhou, X. J. Hu, Z. Zhang and P. Chen, *Synth. Met.*, 2010, **160**, 2481.
83 O. Bubnova, Z. U. Khan, A. Malti, S. Braun, M. Fahlman, M. Berggren and X. Crispin, *Nat. Mater.*, 2011, **10**, 429.
84 Y. M. Sun, P. Sheng, C. A. Di, F. Jiao, W. Xu, D. Qiu and D. B. Zhu, *Adv. Mater.*, 2012, **24**, 932.
85 M. He, L. Zhao, J. Wang, W. Han, Y. L. Yang, F. Qiu and Z. Q. Lin, *ACS Nano*, 2010, **4**, 3241.
86 Y. Y. Wang, J. Zhou and R. G. Yang, *J. Phys. Chem. C*, 2011, **115**, 24418.
87 S. Kuchibhatla, A. S. Karakoti, D. Bera and S. Seal, *Prog. Mater. Sci.*, 2007, **52**, 699.
88 L. D. Hicks and M. S. Dresselhaus, *Phys. Rev. B: Condens. Matter Mater. Phys.*, 1993, **47**, 16631.

89 D. K. Taggart, Y. A. Yang, S. C. Kung, T. M. McIntire and R. M. Penner, *Nano Lett.*, 2011, **11**, 125.
90 Z. Spitalsky, D. Tasis, K. Papagelis and C. Galiotis, *Prog. Polym. Sci.*, 2010, **35**, 357.
91 F. M. Du, R. C. Scogna, W. Zhou, S. Brand, J. E. Fischer and K. I. Winey, *Macromolecules*, 2004, **37**, 9048.
92 R. Gangopadhyay and A. De, *Chem. Mater.*, 2000, **12**, 608.
93 T. Kashiwagi, E. Grulke, J. Hilding, K. Groth, R. Harris, K. Butler, J. Shields, S. Kharchenko and J. Douglas, *Polymer*, 2004, **45**, 4227.
94 C. Yu, Y. S. Kim, D. Kim and J. C. Grunlan, *Nano Lett.*, 2008, **8**, 4428.
95 J. K. Chen, X. C. Gui, Z. W. Wang, Z. Li, R. Xiang, K. L. Wang, D. H. Wu, X. G. Xia, Y. F. Zhou, Q. Wang, Z. K. Tang and L. D. Chen, *ACS Appl. Mater. Interfaces*, 2012, **4**, 81.
96 C. Yu, K. Choi, L. Yin and J. C. Grunlan, *ACS Nano*, 2011, **5**, 7885.
97 D. Kim, Y. Kim, K. Choi, J. C. Grunlan and C. H. Yu, *ACS Nano*, 2010, **4**, 513.
98 T. Koga, X. Sun, S. B. Cronin and M. S. Dresselhaus, *Appl. Phys. Lett.*, 1998, **73**, 2950.
99 T. Koga, X. Sun, S. B. Cronin and M. S. Dresselhaus, *Appl. Phys. Lett.*, 1999, **75**, 2438.
100 B. Paul, V. A. Kumar and P. Banerji, *J. Appl. Phys.*, 2010, **108**, 064322.
101 M. Bachmann, M. Czerner and C. Heiliger, *Phys. Rev. B: Condens. Matter Mater. Phys.*, 2012, **86**, 115320.
102 C. Z. Meng, C. H. Liu and S. S. Fan, *Adv. Mater.*, 2010, **22**, 535.
103 Q. Yao, L. D. Chen, W. Q. Zhang, S. C. Liufu and X. H. Chen, *ACS Nano*, 2010, **4**, 2445.
104 Y. Zhao, G. S. Tang, Z. Z. Yu and J. S. Qi, *Carbon*, 2012, **50**, 3064.
105 G. Kim and K. P. Pipe, *Phys. Rev. B: Condens. Matter Mater. Phys.*, 2012, **86**, 085208.
106 B. Zhang, J. Sun, H. E. Katz, F. Fang and R. L. Opila, *ACS Appl. Mater. Interfaces*, 2010, **2**, 3170.
107 M. Scheele, N. Oeschler, K. Meier, A. Kornowski, C. Klinke and H. Weller, *Adv. Funct. Mater.*, 2009, **19**, 3476.
108 L. Li, Y. W. Yang, X. H. Huang, G. H. Li, R. Ang and L. D. Zhang, *Appl. Phys. Lett.*, 2006, **88**, 103119.
109 Z. B. Zhang, X. Z. Sun, M. S. Dresselhaus, J. Y. Ying and J. Heremans, *Phys. Rev. B: Condens. Matter Mater. Phys.*, 2000, **61**, 4850.
110 H. Yu, P. C. Gibbons and W. E. Buhro, *J. Mater. Chem.*, 2004, **14**, 595.
111 K. C. See, J. P. Feser, C. E. Chen, A. Majumdar, J. J. Urban and R. A. Segalman, *Nano Lett.*, 2010, **10**, 4664.
112 M. Zebarjadi, Z. X. Bian, R. Singh, A. Shakouri, R. Wortman, V. Rawat and T. Sands, *J. Electron. Mater.*, 2009, **38**, 960.
113 M. He, J. Ge, Z. Q. Lin, X. H. Feng, X. W. Wang, H. B. Lu, Y. L. Yang and F. Qiu, *Energy Environ. Sci.*, 2012, **5**, 8351.
114 D. L. Young, T. J. Coutts, V. I. Kaydanov, A. S. Gilmore and W. P. Mulligan, *J. Vac. Sci. Technol., A*, 2000, **18**, 2978.
115 P. Pichanusakorn and P. Bandaru, *Mat. Sci. Eng., R*, 2010, **67**, 19.
116 S. R. Brown, S. M. Kauzlarich, F. Gascoin and G. J. Snyder, *Chem. Mater.*, 2006, **18**, 1873.
117 J. F. Rauscher, C. A. Cox, T. H. Yi, C. M. Beavers, P. Klavins, E. S. Toberer, G. J. Snyder and S. M. Kauzlarich, *Dalton Trans.*, 2010, **39**, 1055.
118 O. Bubnova, M. Berggren and X. Crispin, *J. Am. Chem. Soc.*, 2012, **134**, 16456.
119 J. Sun, M. L. Yeh, B. J. Jung, B. Zhang, J. Feser, A. Majumdar and H. E. Katz, *Macromolecules*, 2010, **43**, 2897.
120 M. Stanford, H. Wang, I. Ivanov and B. Hu, *Appl. Phys. Lett.*, 2012, **101**, 173304.
121 Y. C. Zhang, M. L. Snedaker, C. S. Birkel, X. L. Ji, Y. F. Shi, D. Liu, X. N. Liu, M. M. Moskovits and G. D. Stucky, *Nano Lett.*, 2012, **12**, 1075.